

Mixed Slip-Deceleration PID Control of Aircraft Wheel Braking System

Meng Q. Chen*, Wen S. Liu**, Yun Z. Ma***,
Jian Wang****, Feng R. Xu*****, Ye J. Wang*****

* School of Information Science and Engineering, Central South University, No.932, South Lushan Road, Changsha City, Hunan Province, P.R. China (Tel: 15973130814; e-mail: chenmengqiao@csu.edu.cn).

** Powder Metallurgy Institute, Central South University, No.932, South Lushan Road, Changsha City, Hunan Province, P.R. China (e-mail: liuwensheng@csu.edu.cn)

*** Powder Metallurgy Institute, Central South University, No.932, South Lushan Road, Changsha City, Hunan Province, P.R. China (e-mail: zhuzipm@csu.edu.cn)

**** Powder Metallurgy Institute, Central South University, No.932, South Lushan Road, Changsha City, Hunan Province, P.R. China (e-mail: 605617997@qq.com)

***** School of Information Science and Engineering, Central South University, No.932, South Lushan Road, Changsha City, Hunan Province, P.R. China (e-mail: 329963007@qq.com)

***** Powder Metallurgy Institute, Central South University, No.932, South Lushan Road, Changsha City, Hunan Province, P.R. China (e-mail: 475626974@qq.com)

Abstract: Aircraft antiskid braking system is designed to prevent the main wheels from locking and additionally seeking the optimal braking performance. Wheel deceleration is the traditional controlled target used in antiskid system, since it can be easily measured by angular velocity transducer. However the optimal target value is hard to find due to the changing of road-surface and aircraft velocity. An alternative controlled target is the wheel longitudinal slip which is more robustly controllable under all conditions. But the wheel slip cannot be measured directly, that will definitely result in control error from the poor estimated aircraft speed. In this work a PID control scheme based on mixed slip-deceleration input variable is proposed for aircraft antiskid braking system. This control algorithm is able to stabilize the wheel slip around any equilibrium point. Moreover, it inherits all the appealing characteristics of slip control, while overcoming its sensitivity to slip measurement errors.

Keywords: aircraft antiskid braking system, PID controller, mixed slip-deceleration control, Lyapunov's First Method, aircraft speed influence

1. INTRODUCTION

During the landing run of aircraft, wheel braking system is the main subassembly to dissipate the massive kinetic energy and protect the main wheels from locking that may cause tire excessive wear and even burst (Alsobrook, 1995). While the kinetic energy is dissipated through brake discs, antiskid function of wheel braking system, also known as antiskid braking system, could provide protection for the safety of aircraft by controlling the brake pressure on brake discs. Antiskid function is generally achieved by the antiskid controller, which could determine whether skid happened and then adjust brake pressures to eliminate severe skid of braking wheels (Tanner and Stubbs, 1977).

The traditional controlled variable of antiskid control is the wheel angular velocity or other derived variables such as wheel deceleration, since the wheel angular velocities can be easily measured by the angular velocity transducers mounted inside the wheel axles (Stubbs and Tanner, 1976, Wellstead and Pettit, 1997). However, due to the rapidly changing road-surface and gradually reduced aircraft velocity, it is hard to find the optimal target value. Therefore the on-line estimation or adaptive algorithms are generally used to achieve the most

appropriate target value for improving the performance of speed-based control strategies (Yi *et al.*, 2003).

The wheel longitudinal slip is an alternative variable that be used, since its target value can be set as a constant which is optimal or suboptimal (Johansen *et al.*, 2003, Solyom *et al.*, 2004, Yu, 1997). However, the main drawback of slip control is that the accurate measurement of the longitudinal slip is critical, since the aircraft velocity is unobtainable, considering neither airspeed nor nose wheel speed could precisely represent the aircraft velocity. In the field of automotive brake control, deceleration is introduced to the skid control with weighting coefficient in order to reduce the obnoxious effects of poor slip measurements (Pasillas-Lépine and Loria, 2010, Savaresi, 2005).

The aircraft's force situation and the dynamic process of aircraft landings are much more complicated than automobile. Additionally, the aircraft velocity is larger than that of automobile, whose impact on factors such as tire-road friction coefficient cannot be ignored. In the meantime, the inadequate working conditions of aircraft braking system may increase the slip measurement error, degrading the braking performance. In this paper, we use a convex

combination of the wheel slip and deceleration, named Mixed Slip-Deceleration (MSD), as the controlled variable of aircraft antiskid braking system, in order to acquire good brake performance. We use PID control as the control law, which is very common and mature with antiskid control (Song et al., 2009, Han and Xiao-Ping, 2007). This MSD-PID control algorithm is able to stabilize the wheel slip around any equilibrium point. Moreover, it inherits all the excellent characteristics of slip control, while significantly reducing the troublesome effects of poor slip measurements. We also give precise bounds on the parameters of the control law for which stability is proved mathematically.

2. SYSTEM DESCRIPTION

The aircraft structure with tricycle-type telescopic landing gears is typically used for the design and testing of braking control algorithms. The model is given by the following set of equations:

$$\begin{cases} J\dot{\omega} = r\mu_1 N_1 - T_b \\ m\dot{v} = -4\mu_1 N_1 - 2\mu_2 N_2 + F_v - k_x v^2 \\ 4N_1 + 2N_2 = mg - k_y v^2 \\ 4\mu_1 N_1 H + 4N_1 a + 2\mu_2 N_2 H - 2N_2 b = 0 \end{cases} \quad (1)$$

where ω is the wheel angular speed; v is the longitudinal speed of the aircraft body; N_1 and N_2 are the vertical loads at the contact points of main wheels and nose wheels; μ_1 and μ_2 are the tire-road friction coefficients of main wheel and nose wheel; T_b is the braking torque on braking discs; F_v is the engine residual thrust; k_x and k_y are the coefficient of air resistance in horizontal and vertical; H is the height of the center of aircraft gravity; a and b are the horizontal distance from the center of aircraft gravity to main wheels and nose wheels; and J , r , m and g are the momentum of inertia of the main wheel, the main wheel radius, the aircraft mass, and the gravitational acceleration, respectively.

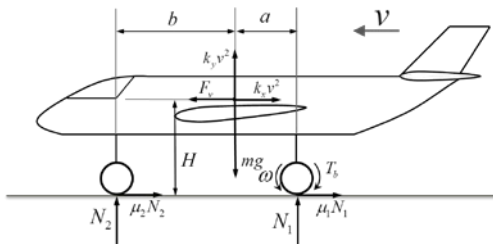


Fig. 1. Dynamical model of aircraft during braking process.

The deceleration η used in this paper is defined as a normalized linear wheel deceleration, and wheel slip λ is also defined as follow:

$$\begin{cases} \eta = -\frac{\dot{\omega}r}{g} \\ \lambda = \frac{v - \omega r}{v} \end{cases} \quad (2)$$

Observing the first two equations of (1), the system dynamic characteristic is affected by the vertical loads on wheels N_i

and the tire-road friction coefficients μ_i . According to the Dynamic balance equations of aircraft, given in the last two equations of (1), N_i can be analytically described as follow:

$$\begin{cases} N_1 = \frac{1}{4} \frac{b - \mu_2 H}{a + b + (\mu_1 - \mu_2)H} (mg - k_y v^2) \\ N_2 = \frac{1}{2} \frac{a + \mu_1 H}{a + b + (\mu_1 - \mu_2)H} (mg - k_y v^2) \end{cases} \quad (3)$$

Noted that N_i is also affected by μ_i , it is crucial to study the accurate model of μ_i . However the tire-road friction coefficient μ_i depends on a large number of features of the road, tire, speed, and the depth of slip, a simple empirical model is widely used:

$$\mu(\lambda; \theta_j) = \theta_1 \sin(\theta_2 \cdot \arctg(\theta_3 \cdot \lambda)) \quad (4)$$

The parameters θ_j are decided by tire conditions, road conditions, and aircraft velocity. To simplify the analysis and design process, we approximately consider the tire-road contact conditions and aircraft velocity remain unchanged during every short time periods of the rotational dynamic process of wheels.

Plugging the expression $\dot{\lambda} = -\frac{r}{v}\dot{\omega} + \frac{r\omega}{v^2}\dot{v}$ derived from (2) into (1), we can obtain the following equation:

$$\begin{aligned} \dot{\lambda} = - \left[\left(\frac{r^2}{vJ} + \frac{4(1-\lambda)}{mv} \right) \mu_1(\lambda) N_1 + \frac{2(1-\lambda)}{mv} \mu_2(\lambda) N_2 \right] \\ + \frac{rT_b}{vJ} + \frac{(1-\lambda)T_v}{mv} - \frac{v(1-\lambda)k_x}{m} \end{aligned} \quad (5)$$

By replacing $\eta = -\frac{\dot{\omega}r}{g}$ into (1), we obtain the expression:

$$\eta = -\frac{r}{gJ} (r\mu_1(\lambda)N_1 - T_b) \quad (6)$$

With the purpose of controlling the depth of skid or the deceleration of wheel, we should study the dynamic relations between the system input instruction T_b and the output λ or η . Equations in (5) and (6) can be expressed as followed:

$$\begin{cases} \dot{\lambda} = \phi(\lambda) + \gamma T_b \\ \eta = \varphi(\lambda) + \xi T_b \end{cases} \quad (7)$$

It is easy to observe that the system is nonlinear, so we can hardly analysis the global dynamic of system. Based on the theory of Lyapunov's First Method, the problem can be transformed into the dynamic characteristics analysis around some equilibrium point. Firstly, the quasi-linear system model is constructed as followed:

$$\begin{cases} \Delta \dot{\lambda} = \phi'_{(\bar{\lambda})} \Delta \lambda + \gamma \Delta T_b \\ \Delta \eta = \varphi'_{(\bar{\lambda})} \Delta \lambda + \xi \Delta T_b \end{cases} \quad (8)$$

Then the dynamic characteristics analysis methods of linear systems can be applied in this model.

3. MODEL ANALYSIS

Based on the analysis of the previous section, the wheel dynamics is presented by the first-order approximation mode (see equation (8)) around the equilibrium point $\bar{\lambda}$. The significant equilibrium point should share the characteristic of $\dot{\lambda}=0$ and $\eta=\bar{\eta}$. Combined with the above equations, we can obtain the following relation between $\bar{\eta}$ and $\bar{\lambda}$:

$$\bar{\eta} = (1 - \bar{\lambda}) \left(\frac{4\mu_1(\bar{\lambda})N_1 + 2\mu_2N_2 - F_v + k_x v^2}{mg} \right)$$

Therefore, the transfer function $G_\lambda(s)$ from δT_b to $\delta\lambda$ around the equilibrium points $\bar{\lambda}$ is given by:

$$G_\lambda(s) = \frac{\delta\lambda}{\delta T_b} = \frac{\gamma}{s - \phi'_{(\bar{\lambda})}} = \frac{\frac{r}{vJ}}{s + \left\{ \left[\frac{r^2}{vJ} + \frac{4(1-\bar{\lambda})}{mv} \right] \mu_1'(\bar{\lambda})N_1 - \frac{4\mu_1(\bar{\lambda})N_1 + 2\mu_2N_2 - T_v + vk_x}{mv} + \frac{vk_x}{m} \right\}} \quad (9)$$

Consider that the nose wheels are in the state of pure roll with no brake applied, the tire-road friction coefficient μ_2 is approximately defined as a constant. The transfer function $G_\eta(s)$ from δT_b to $\delta\eta$ is obtained by:

$$G_\eta(s) = \frac{\delta\eta}{\delta T_b} = \phi'_{(\bar{\lambda})} \frac{\delta\lambda}{\delta T_b} + \xi = \frac{r}{gJ} \left\{ s + \left[\frac{4(1-\bar{\lambda})}{mv} \right] \mu_1'(\bar{\lambda})N_1 - \frac{4\mu_1(\bar{\lambda})N_1 + 2\mu_2N_2 - T_v + vk_x}{mv} + \frac{vk_x}{m} \right\} \quad (10)$$

The open-loop dynamic characteristics around the equilibrium point can be easily analyzed. Having the same pole, the stability condition for $G_\lambda(s)$ and $G_\eta(s)$ is:

$$\left[\frac{r^2}{vJ} + \frac{4(1-\bar{\lambda})}{mv} \right] \mu_1'(\bar{\lambda})N_1 - \frac{4\mu_1(\bar{\lambda})N_1 + 2\mu_2N_2 - T_v + vk_x}{mv} > 0$$

Modify the inequation into the following expression:

$$\mu_1'(\bar{\lambda}) > \frac{4\mu_1(\bar{\lambda}) + 2\mu_2 N_2/N_1 + T_v/N_1 - k_x v^2/N_1}{\left[\frac{mr^2}{J} + 4(1-\bar{\lambda}) \right]}$$

Since $\frac{mr^2}{J} + 4(1-\bar{\lambda})$ is much larger than each item in the

polynomial of numerator, it can be reduced to $\mu_1'(\bar{\lambda}) > 0$. This means the open-loop system is unstable around the equilibrium point $\bar{\lambda}$ beyond the peak of $\mu_1(\lambda)$.

The minimum-phase condition for $G_\eta(s)$ is:

$$\mu_1'(\bar{\lambda}) > \frac{4\mu_1(\bar{\lambda}) + 2\mu_2 N_2/N_1 + T_v/N_1 - k_x v^2/N_1}{4(1-\bar{\lambda})}$$

It can be easily analyzed that the open-loop dynamic properties are affected by the equilibrium point $\bar{\lambda}$. The

pilots cannot guarantee the stability of system under all conditions without any supplementary control method. The antiskid braking system is mainly designed for this fundamental objective.

4. CONTROL STRATEGIES

The structure of Mixed Slip-Deceleration (MSD) control scheme is outlined in Fig. 2. The basic idea is to define an control variable ε , which is the convex combination of the two measured variables λ and η , namely:

$$\varepsilon = \alpha\lambda + (1-\alpha)\eta, \quad \alpha \in [0,1] \quad (11)$$

and to regulate the output variable to a target value $\bar{\varepsilon}$. This reference value $\bar{\varepsilon}$ can be a set-point constant value as the convex combination of slip and deceleration, namely $\bar{\varepsilon} = \alpha\bar{\lambda} + (1-\alpha)\bar{\eta}$, or a variational value adapted to different factors.

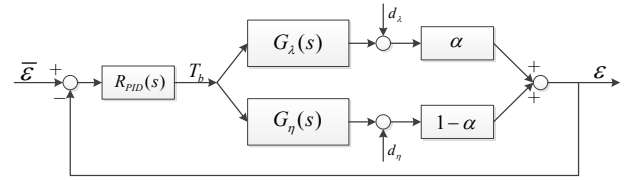


Fig. 2. General structure of MSD controller.

The control variable T_b is assumed to be driven by the regulation error through a simple PID controller, since PID controller is commonly used in SISO first-order linear systems, and also satisfactorily applied to actual aircraft brake controllers. The PID controller is complemented with a first-order filter to achieve approximation of the ideal derivative term, the transfer function is given as follow:

$$R_{PID}(s) = K \frac{(\tau_1 s + 1)(\tau_2 s + 1)}{s(Ts + 1)}, \quad T > 0, \quad \tau_1 > 0, \quad \tau_2 > 0$$

The dynamic characteristics change a lot with the variation of weight value α from 1 to 0. The two extremal cases of MSD controller are exactly the slip controller ($\alpha=1$) and the deceleration controller ($\alpha=0$). Pondering the geometrical relationship between the controlled variable plot and $\eta-\lambda$ curve in Fig. 3, we can guarantee the existence and uniqueness of the steady-state equilibrium point by carefully choosing $\bar{\varepsilon}$ and α .

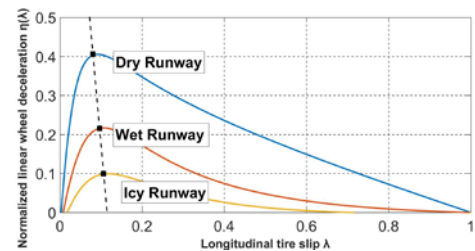


Fig. 3. Graphical interpretation of MSD control in the (λ, η) domain for different road condition.

The open-loop transfer function $G_\varepsilon(s)$ from δT_b to $\delta\varepsilon$ is given by:

$$G_\varepsilon(s) = \frac{\delta\varepsilon}{\delta T_b} = \frac{(1-\alpha) \frac{r}{gJ} \left[s + \left[\frac{4(1-\bar{\lambda})}{mv} \mu_1'(\bar{\lambda}) N_1 - \frac{4\mu_1(\bar{\lambda}) N_1 + 2\mu_2 N_2}{mv} - \frac{T_v}{mv} + \frac{vk_x}{m} + \frac{\alpha g}{(1-\alpha)v} \right] \right]}{s + \left[\frac{r^2}{vJ} + \frac{4(1-\bar{\lambda})}{mv} \right] \mu_1'(\bar{\lambda}) N_1 - \frac{4\mu_1(\bar{\lambda}) N_1 + 2\mu_2 N_2}{mv} - \frac{T_v}{mv} + \frac{vk_x}{m}} \quad (12)$$

And $G_\varepsilon(s)$ can be modified to the following form:

$$G_\varepsilon(s) = \frac{C(S+A'')}{S+A}$$

$$\text{where } C = (1-\alpha) \frac{r}{gJ}, \quad A'' = A - \frac{r^2}{vJ} \mu_1'(\bar{\lambda}) N_1 + \frac{\alpha g}{(1-\alpha)v},$$

$$A = \left[\frac{r^2}{vJ} + \frac{4(1-\bar{\lambda})}{mv} \right] \mu_1'(\bar{\lambda}) N_1 - \frac{4\mu_1(\bar{\lambda}) N_1 + 2\mu_2 N_2}{mv} - \frac{T_v}{mv} + \frac{vk_x}{m}$$

So the closed-loop transfer function of the Mixed Slip-Deceleration control system is obtained:

$$L_\varepsilon(s) = \frac{R_{pid}(s)G_\varepsilon(s)}{1+R_{pid}(s)G_\varepsilon(s)} = \frac{\tau_1\tau_2 KCs^3 + [KC(\tau_1+\tau_2) + \tau_1\tau_2 KCA'']s^2 + [KC + (\tau_1+\tau_2)KCA']s + KCA'}{(T + \tau_1\tau_2 KC)s^3 + [1+TA + KC(\tau_1+\tau_2) + \tau_1\tau_2 KCA'']s^2 + [A + KC + (\tau_1+\tau_2)KCA']s + KCA'} \quad (13)$$

The necessary and sufficient condition for closed-loop stability of system is obtained:

$$\begin{cases} T + KC\tau_1\tau_2 > 0 \\ 1 + TA + KC(\tau_1 + \tau_2) + KC\tau_1\tau_2 A'' > 0 \\ A + KC + KC(\tau_1 + \tau_2)A'' > 0 \\ KCA'' > 0 \\ [1 + TA + KC(\tau_1 + \tau_2) + KC\tau_1\tau_2 A''] \cdot [A + KC + KC(\tau_1 + \tau_2)A''] - (T + KC\tau_1\tau_2) \cdot KCA'' > 0 \end{cases}$$

Analyzing the inequations above, we can easily find a value \bar{K} such that, for $K > \bar{K}$, the stability condition is satisfied, when the coefficients of K and the quadratic coefficient of polynomial are positive. So the following condition is obtained:

$$\begin{cases} \tau_1 + \tau_2 + \tau_1\tau_2 A'' > 0 \\ 1 + (\tau_1 + \tau_2)A'' > 0 \\ A'' > 0 \\ 1 + (\tau_1 + \tau_2)A'' + \tau_1\tau_2 A''^2 > 0 \end{cases}$$

simplified to the inequation $A'' > 0$.

Having $A' = A - \frac{r^2}{vJ} \mu_1'(\bar{\lambda}) N_1$ (consider aircraft speed v as a

scaling constant), we can obtain the worst condition of the inequation: $(A'v)_{Min} + \frac{\alpha g}{(1-\alpha)} > 0$.

So the condition of α is derived:

$$\alpha > \frac{(A'v)_{Min}}{(A'v)_{Min} - g}$$

In order to satisfy the stability requirement in every condition with a fixed value of α , the minimum of α is given as:

$$\alpha_{Min} = \left[\frac{(A'v)_{Min}}{(A'v)_{Min} - g} \right]_{Max} \quad (14)$$

The advantage of Mixed Slip-Deceleration control strategy is obvious that by choosing a proper value of α in the range of $\alpha_{Min} < \alpha < 1$, the reliance and sensitivity on wheel slip is reduced. Meanwhile we can obtain a unique steady-state equilibrium point and the global stability of MSD control system can be guaranteed with sufficiently large controller parameter K , namely $K > \bar{K}$. Sharing the same features of slip control strategy, the MSD control also has other advantages that will be discussed in the next section.

5. DISTURBANCE ANALYSIS

Relying on the wheel slip and deceleration, MSD control is sensitive to the value variation of λ and η . It is indispensable to analyze the effects of controlled signal disturbance on the control performance. Based on the structure of MSD controller in Fig.2, the disturbance term $d_\varepsilon(\alpha)$ of control variable ε has a relationship with the slip and deceleration disturbances λ and η :

$$D_\varepsilon(s) = [\alpha D_\lambda(s) + (1-\alpha)D_\eta(s)]S_\varepsilon(s)$$

where $D_\varepsilon(s)$, $D_\lambda(s)$, $D_\eta(s)$ are the Laplace transforms of the disturbance signals $d_\varepsilon(\alpha)$, d_λ , d_η respectively, and $S_\varepsilon(s)$ is the closed-loop sensitivity function, given by:

$$S_\varepsilon(s) = \frac{1}{1+G_\varepsilon(s;\alpha) \cdot R_{pid}(s)} = \frac{Ts^3 + [1+TA]s^2 + As}{(T + \tau_1\tau_2 KC)s^3 + [1+TA + KC(\tau_1 + \tau_2) + \tau_1\tau_2 KCA'']s^2 + [A + KC + (\tau_1 + \tau_2)KCA']s + KCA'}$$

For the purpose of comparing the disturbance resisting capacity of slip control and MSD control, we also deduce the sensitivity function of slip control:

$$S_\lambda(s) = \frac{1}{1+G_\lambda(s;\alpha) \cdot R_{pid}(s)} = \frac{Ts^3 + [1+TA]s^2 + As}{Ts^3 + (1+TA + KB\tau_1\tau_2)s^2 + [A + KB(\tau_1 + \tau_2)]s + KB}$$

where $B = \frac{r}{vJ}$.

It can be easily analyzed that the frequency characteristic of these two functions is related to the value of aircraft speed v , wheel slip λ and weight factor α . Assigning the control parameter as $K=6 \times 10^6$, we can obtain the Bode-plots of closed-loop sensitivity function of MSD and slip control for different conditions, namely aircraft speed $v=10m/s$, wheel slip $\lambda=0.05$ or 0.2 , weight factor $\alpha=0.9$ or 1 in Fig. 4. In this condition, all of the system closed-loop poles have negative real parts, which guarantee the stability of system. The low frequency gain decreases no matter what the slip and weight factor value. The high frequency gain strongly decreases in MSD control system when $\alpha=0.9$, while remains unchanged in slip control system ($\alpha=1$).

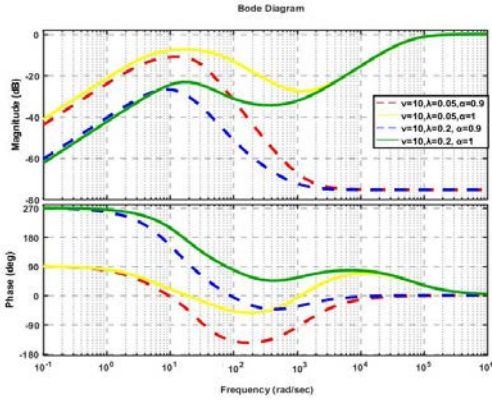


Fig. 4. Bode-plots of closed-loop sensitivity function of MSD and slip control for $K=6 \times 10^6$

The analysis above has shown the noise-attenuation effect of MSD control strategy is obviously stronger than that of slip control. Meanwhile MSD control guarantees the uniqueness of steady-state equilibrium point with respect to deceleration control. These advantages make the MSD control an admirable control strategy for aircraft braking control system.

6. INFLUENCE OF AIRCRAFT SPEED

The biggest difference between aircraft and automobile is that the aircraft braking process can be easily influenced by aerodynamic forces and tire-road friction force which all have connections with aircraft speed. In the previous discussion we assume that the aircraft speed remains unchanged during every short time periods of the rotational dynamic process of wheels. However, the scale of aircraft speed still determines the instantaneous system model, which affecting the stability and control performance of closed-loop system. The influence of aircraft speed is analyzed for the following aspects

6.1 Control Target

As mentioned above, the tire-road friction coefficients μ_i depends on a large number of features of road, tire and aircraft speed. The aircraft speed strongly affects the shape of $\mu(\lambda; \theta_j)$ curve, the vertical loads N_1 and N_2 and the air resistance term $k_x v^2$, hence affecting the figure of deceleration-slip ($\eta-\lambda$) curve, under the relation :

$$\bar{\eta} = (1 - \bar{\lambda}) \left(\frac{4\mu_1(\bar{\lambda})N_1 + 2\mu_2N_2 - F_v + k_x v^2}{mg} \right)$$

Analyzing the $\eta-\lambda$ curve at different aircraft speeds, it is easy to observe that the peak point of each curve is shifting non-linearly, see Fig. 5, the impact of aircraft speed on the tire-road friction coefficients has been considered. Therefore, some performance of MSD control strategy is sacrificed for the fixed structure, since the target point (where the line $\bar{\varepsilon} = \alpha\bar{\lambda} + (1-\alpha)\bar{\eta}$ and the curve $\bar{\eta}(\bar{\lambda})$ intersect) is more far away from optimal point. This issue can be dealt with an adaptive modification with control variable

$\bar{\varepsilon} = \alpha\bar{\lambda} + (1-\alpha)\bar{\eta}$ concerning aircraft speed that will be discussed in the future work.

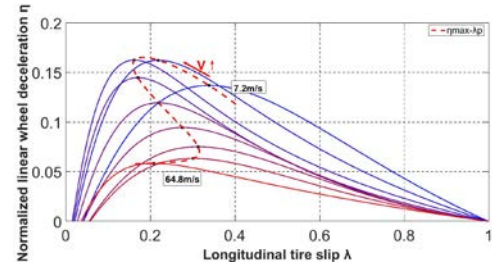


Fig. 5. Variation trend of maximum points of wheel deceleration.

6.2 System dynamic characteristics

The stability of MSD method is related to the values of control parameters (α and K). While the value range of each parameter is affected by aircraft speed v . In last section the minimum value of α was given as function (14), which has ignored the influence of aircraft speed v on the variable A' . Analyzing the stable condition of MSD control, we can obtain the general expression of α :

$$(g - A'v)\alpha > -A'v.$$

Setting the function of slip $\bar{\lambda}$ and aircraft speed v as $F(\bar{\lambda}; v) = A'v - g$, it is easy to derive the worst situation when the value of $F(\bar{\lambda}; v)$ is minimum:

$$\alpha_{Min} = P = \frac{F(\bar{\lambda}; v)_{Min} + g}{F(\bar{\lambda}; v)_{Min}}$$

The minimum of α can be easily figured out that $\alpha_{Min} = 0.46$ with $F(\bar{\lambda}; v)_{Min} = -18.18$ (when $\lambda=0.18$ and $v=0$). As the aircraft speed increases, the value of $F(\bar{\lambda}; v)$ increases that leads the range of α becoming larger. Therefore, as long as the condition of $\alpha_{Min} < \alpha \leq 1$ is satisfied, it is easy to find a constant \bar{K} such that, for $K > \bar{K}$, the stability condition of MSD control is guaranteed under any slip and aircraft speed situation. Simultaneously, the value of \bar{K} could be affected by slip ratio $\bar{\lambda}$ and aircraft speed v , but we will not amplify the numerical calculation here. We usually choose the control parameter $K > \bar{K}$ sufficiently large enough so that it can satisfy all conditions.

7. NUMERICAL SIMULATION

The aircraft braking system dynamical model used above has been simplified to a certain degree, in order to focus on the very bulk of the control problem and to gain a deep insight in the algorithm behaviour, while remaining the main dynamical features of the system. However, the theoretical analysis based on this simplified model should be corroborated by more reliable simulation results.

A detailed aircraft braking simulator is constructed in MATLAB/SIMULINK and tuned to fit the characteristics of a certain type aircraft. The simulation results can be considered very close to real situation. Specifically, the simulator has been complemented with the dynamics of direct drive press servo-valve (second-order object) and oil pipeline (inertial element), which can be approximated as follows:

$$G_{actuator}(s) = \frac{1}{0.00318s^2 + 0.0406s + 1} \cdot \frac{1}{0.01s + 1}$$

The slip controller and MSD controller have been both implemented with a PID control architecture (complemented with incomplete derivation), which have been tuned to work satisfactorily in every working condition, obtaining the following transfer function:

$$R_{PID}(s) = 149 \frac{(0.0199s + 1)(2.012s + 1)}{s(0.02s + 1)}$$

Before evaluating the noise sensitivity of the control scheme, we should analyze the measurement noises of the wheel deceleration and wheel slip, which are shown in Fig. 6. Due to poor speed estimation, the measurement noise of wheel slip d_λ has larger variance than d_η while characterized by huge spikes at the same time. In Fig. 7 the behaviours of the wheel slip of slip and MSD control are compared (on dry asphalt with measurement noises). Same as expected, the noise sensitivity of MSD control is remarkably lower than slip control, the actual wheel slip is more stable around control target and the slipping is less serious at low speed, leading to better braking action. The brake efficiency of MSD control has reached 85%, while that of slip control is still 81.5%. This result well proves the reliability of theoretical analysis which is worked out in the simplified setting.

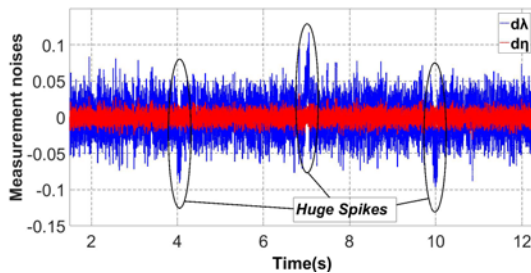


Fig. 6. Measurement noises of the wheel deceleration and wheel slip

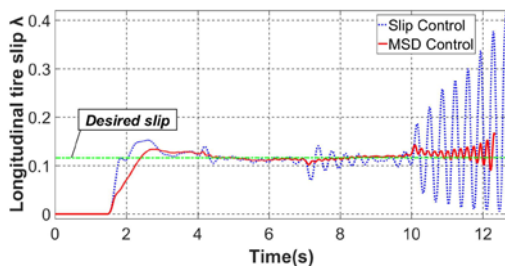


Fig. 7. Slip behaviour of Slip control and MSD control under measurement noises

8. CONCLUSIONS

In this paper, a PID control scheme based on mixed slip-deceleration input variable has been proposed for aircraft antiskid braking system. This control algorithm is able to stabilize the wheel slip around any equilibrium point. Moreover, it inherits all the appealing characteristics of slip control, while overcoming its sensitivity to slip measurement errors. The brake efficiency of the method is higher than slip control, resulting in a better braking performance. The influence of aircraft velocity has also been demonstrated, which restricts the range of control parameters.

REFERENCES

- Alsobrook, C.B. (1995). Wear of F-16 Mainwheel Tires During Constant Slip Braking. *SAE Technical Paper*.
- Han, Y.H., and Xiao-Ping, M.A. (2007). Application of fuzzy PID controller in the electric brake system of aircraft. *Aeronautical Computing Technique*, 37(5), 103-105.
- Johansen, T.A., Petersen, I., Kalkkuhl, J., and Lüdemann, J. (2003). Gain-scheduled wheel slip control in automotive brake systems. *IEEE Transactions on Control Systems Technology*, 11(6), 799-811.
- Pasillas-Lépine, W., and Loría, A. (2010). A new mixed wheel slip and acceleration control based on a cascaded design. *IFAC Proceedings Volumes*, 43(14), 879-884.
- Stubbs, S.M. and Tanner, J.A. (1976). Behavior of aircraft antiskid braking systems on dry and wet runway surfaces: A velocity-rate-controlled, pressure-bias-modulated system. *NASA Langley Research Center, Virginia*.
- Solyom, S., Rantzer, A., and Lüdemann, J. (2004). Synthesis of a Model-Based Tire Slip Controller. *Vehicle System Dynamics*, 41(6), 475-499..
- Savaresi, S.M., Tanelli, M., Cantoni, C., Charalambakis, D., Previdi, F., and Bittanti, S. (2005). Slip-deceleration control in anti-lock braking systems. *IFAC Proceedings Volumes*, 38(1), 103-108.
- Song, H., Fang, B., and Wang, P. (2009). Research and Applications of Immune PID Adaptive Controller in Anti-Skid Braking System for Aircraft. *International Conference on Information Engineering and Computer Science* (pp.1-5). IEEE.
- Tanner, J.A. and Stubbs, S.M. (1977). Behavior of aircraft antiskid braking systems on dry and wet runway surfaces: A slip-ratio-controlled system with ground speed reference from unbraked nose wheel. *NASA Langley Research Center, Virginia*.
- Wellstead, P.E. and Pettit, N.B.O.L. (1997). Analysis and redesign of an antilock brake system controller. *IEE Proceedings - Control Theory and Applications*, 144(5), 413-426.
- Yu, J.S. (1997). A robust adaptive wheel-slip controller for antilock brake system. *Proceedings of the IEEE Conference on Decision and Control*, Vol.3, 2545-2546.
- Yi, J., Alvarez, L., Claeys, X., and Horowitz, R.(2003). Emergency braking control with an observer-based dynamic tire/road friction model and wheel angular velocity measurement. *Vehicle system dynamics*, 39(2): 81-97.